

Computer-Aided Detection of Gastrointestinal Disorders with Endoscopy Capsule Images

Diogo D.^{*1,2}, Moreira R.^{†1}, Gonçalves G.¹, Faria L.²

¹Research and Technology Department, INOVA+, Porto, Portugal

²Department of Informatics Engineering, Polytechnic of Porto - School of Engineering (ISEP), Porto, Portugal

*daniela.a.s.diogo@hotmail.com; †rita.moreira@inovamais.pt

Abstract-The endoscopy capsule (EC) is a reliable, secure, and non-invasive tool for diagnosing disorders in the gastrointestinal tract (GIT). To aid in early detection diagnostic efficiency for various disorders in difficult-to-reach areas of the GIT, the authors developed the PhotonicPill EC. This EC uses photonics technology to facilitate a more accurate and timely diagnosis of various pathologies. The main objective of this research project was to develop a clinical decision support system that uses EC-acquired data for the early identification of bleeding and polyps, and for the detection of vascularization inside the GIT. The bleeding detection method was based on the evaluation of minimum and maximum values for each RGB (red-green-blue) channel, combined with morphological and local operations. Regarding the polyp detection method, segmentation was accomplished with a marker-controlled watershed transform, using measures related to the typical shape of a polyp for decision purposes. The vascularization detection algorithm used the calculation of maximum values for each channel to select a maximum threshold value for segmentation of the vascularization area. For validation of the developed methods, the EC images with known diagnoses were used as ground truth. The results showed very satisfactory percentages of classification, which fulfilled the objective for bleeding, polyps, and vascularization detection.

Keywords- Endoscopy Capsule; Bleeding; Early Detection; Polyps; Image Processing; Photonic Pill

I. INTRODUCTION

According to World Health Organization data, colorectal cancer was responsible for 694,000 deaths in 2012 [1]. Effective treatments for this type of cancer require early detection, which can only be achieved with frequent clinical examinations. Developed from the need for a less invasive diagnostic method, the EC is a reliable, safe, and non-invasive device that allows the visualization of the whole GIT. In fact, the endoscopy capsule was created to complement traditional diagnostic methods (endoscopy and colonoscopy) that are too invasive for frequent examinations [2-4] since these procedures are painful and unpleasant for the patient due to the size of the equipment or wiring and require sedation and hospitalization. However, EC devices also have some disadvantages including battery life limitations, the impossibility to analyze the same area for long periods of time, and image noise-related acquisition problems. Nevertheless, constant technological advances are being utilized to solve these shortcomings. Thus, the EC can be considered a recent major technological breakthrough in medicine, which promotes the early diagnosis of many gastrointestinal diseases, such as colorectal cancer, since it allows the study of the entire GIT with records of image data for further analysis.

The authors developed a new EC, the PhotonicPill, which is comprised of a set of modules based on photonics to allow a more accurate and timely diagnosis of various disorders, such as polyps and bleeding, as well as the possibility of therapeutic interventions in the difficult-to-access regions of the GIT. This EC uses narrow band imaging (NBI) technology to improve diagnosis methods and a technique of photodynamic therapy (PDT) for therapeutic purposes.

NBI is an optical imaging technology that improves the visibility of blood vessels and other tissues on mucosal surfaces. This optical imaging technology is based on the physical principle that the depth of penetration of the light wave in tissue is directly proportional to its wavelength; thus, the higher the wavelength, the greater the tissue penetration [5]. Blue light with a wavelength of 415 nm is particularly useful for the detection of tumors, which are often highly vascularized. On the other hand, green light with a 540 nm wavelength highlights sub-epithelial vessels since it penetrates deeper than blue light. Precancerous lesions are developed in the superficial layer of the GIT, meaning the structure of the blood vessels is altered in that area [6, 7].

Computational techniques of automatic image processing and analysis can be used to facilitate the detection of these conditions and homogenize responses between medical professionals, since each EC examination acquires about 58,000 images of the entire GIT. To facilitate the analysis of such large amounts of data, image-processing techniques can be used to identify the existence of disorders within the GIT. In this manner, it is possible to support the early diagnosis of these diseases, as well as reduce physicians' fatigue and increase their performance and efficiency in data analysis.

The work presented in this article aimed to develop clinical software to support the analysis and management of data acquired with the PhotonicPill EC; however, this software can also be used with others ECs. The software was developed to provide an intuitive tool for physicians to manage patients' records and all the data acquired with the EC, as well as automatically detect the presence of bleeding or polyps in the EC images to assist the physician in the diagnosis of GIT

disorders. Furthermore, this software allows the detection of vascularization in NBI images and the tridimensional (3D) reconstruction of gastrointestinal mucosa to assess the shape of protrusions.

II. METHODS

A. Bleeding Detection

One of the most relevant aspects for bleeding detection is the color difference presented as the result of this disorder within the GIT. The GIT contains very similar patterns and shades of red in some parts; this disorder has features of differentiation, such as high saturation and low brightness. Thus, a method was developed to automatically detect bleeding inside the GIT based on color features. Fig. 1 presents a flowchart illustrating the main steps of the developed method.

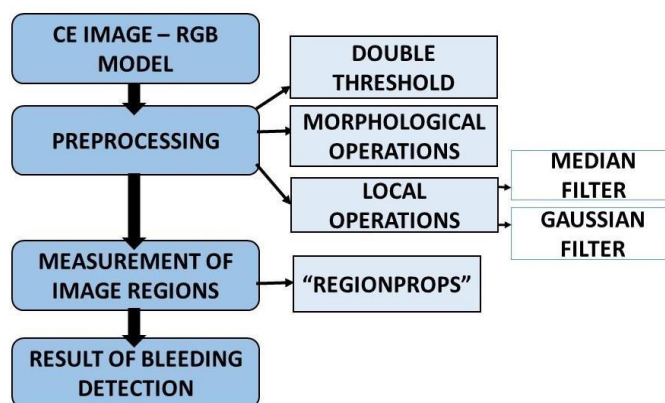


Fig. 1 Flowchart of the developed bleeding detection method

Initially, pre-processing starts with the empirical detection of minimum and maximum values for each channel R (red), G (green), and B (blue). For this purpose, a total of 21 images containing bleeding were used. With the definition of these values, the average was calculated and a double threshold was defined for segmentation of the bleeding area. After this segmentation in the EC image, it was observed that the resulting binary image was noisy around the area of interest, which was removed by applying smoothing techniques. As such, a median filter with a 3x3 kernel and Gaussian filter with sigma (σ) 2 in a 3x3 square matrix were used. Subsequently, a morphological open operation was applied with a 3x3 square structuring element.

After this smoothing process, the resulting image still presented some noise, as traduced by the presence of small areas irrelevant to the study, as can be seen in Fig. 2A. Therefore, to remove this noise, a threshold based on the area was used. For that purpose, the connectivity between pixels (connectivity 4) was calculated in order to split the image into different blobs according to the various objects. In this way, it was possible to calculate the individual area of each blob. Noise zones visible in Fig. 2B are characterized by their unusual and small shapes. Thus, by performing a quantitative analysis, it was discovered that the noise blobs correspond to areas with a value lower than 60 pixels. With this threshold, these small areas were removed and it was possible to obtain a more reliable segmentation result, as can be seen in Fig. 2C.

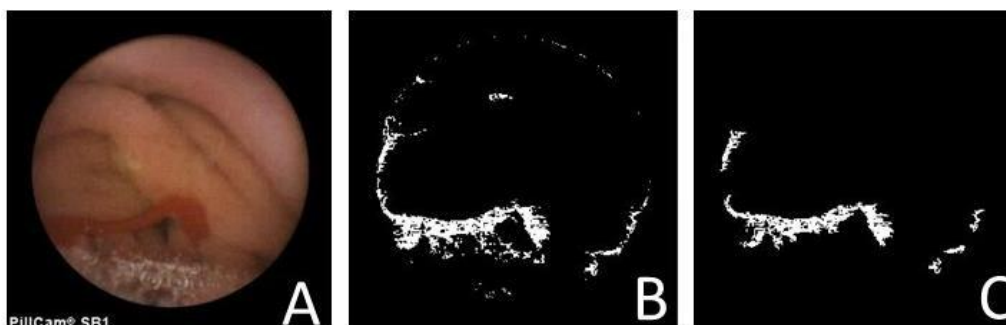


Fig. 2 Bleeding detection: A) Original image; B) Image after segmentation of the region of interest with noise; C) Image after noise removal

After the segmentation process and noise removal, the next step was to decide if it corresponded to a bleeding zone. To do this, the remaining objects in the binary image were computed, and it was observed that the largest area coincided with the bleeding area. Because the goal was to detect potential pixels corresponding to bleeding, a limit area value of 199 pixels was defined, where there would be a high probability of the image containing blood, and therefore automatically indicated as a bleeding zone.

B. Polyp Detection

Polyp detection in EC images is mainly based on volume and form measures, since these are characteristics that distinguish these anomalies from the rest of the GIT. The method proposed in this work was based on these features, and can be organized as a sequence of a few high-level operations: image pre-processing, polyp segmentation and classification, and 3D reconstruction for shape analysis (Fig. 3).

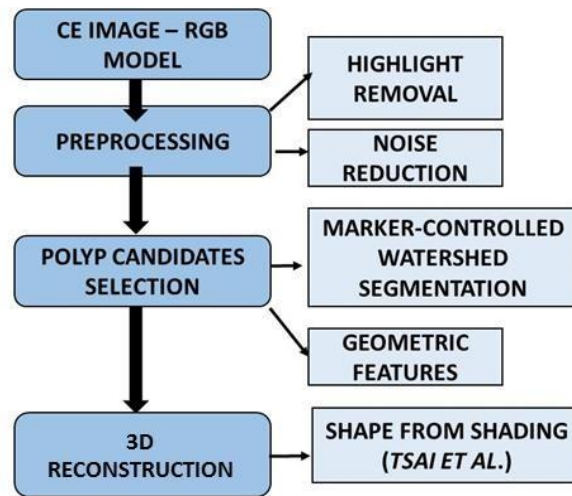


Fig. 3 Flowchart of the developed polyp detection method

Firstly, pre-processing starts with the removal of image highlights, which are linear combinations of specular and diffuse reflection components. Since the majority of digestive endoscopy structures are not homogeneous, some areas reflect back immediately when the light falls on them, creating a specular reflection, while the rest of the light beams penetrate the object and then reflect back, creating a diffuse reflection. The presence of specular reflection can interfere with image processing and the final 3D reconstruction; therefore, these highlights must be removed. For this purpose, the method of Mallick, *et al.* [8] is used to detect and remove the highlights and an inpainting technique applied to fill these areas. For smoothing and noise reduction, a median filter is computed (5x5).

Subsequently, for polyp segmentation, a marker-controlled watershed technique is used. In EC images, a polyp is often characterized by different colors (or intensities) depending on the relative distance between the polyp and the light source. This distance varies since the polyp is a spherical 3D structure, meaning it is usually outlined by a sharp edge. In this way, the use of a watershed algorithm is a good option for polyp segmentation due to its ability to detect edges in a highly effective manner.

This algorithm uses a topological aid function with edge representation as input, usually the magnitude of the image gradient, along with foreground and background markers that act as initial points for segmentation. For this purpose, a k-means algorithm [9] was applied, which resulted in various segmented regions based on their level of elevation, as can be seen in Fig. 4B. By selecting the local maxima it was possible to obtain the foreground markers (Fig. 4C). To detect the background markers, the Otsu global threshold method was used to perform a rough segmentation of the k-means image. Then, a skeleton of the background was obtained to outline the foreground markers by computing the watershed transform of the distance transform of the image with the foreground markers. Finally, the gradient of the original image was modified to include the previously obtained markers (Fig. 4E) and the watershed transform of this image was calculated (Fig. 4F). As can be seen, the result of the watershed segmentation divided the image into various zones according to the boundaries found, within which was delimited to the polyp.

In general, polyps have a circular or elliptical shape; therefore, geometric information can be useful for polyp classification. Since the watershed transform segments the image into several blobs, geometrical features for each blob should be computed to verify whether it is a polyp candidate. For this purpose, a pre-selection of blobs is initially made using a double threshold of the area. Very large (>20,000 pixels) or very small (<500 pixels) blobs are not considered as the images have an average size of 288x288 pixels. To evaluate the shape of the blob and its approximation to a circular or elliptical form, three different parameters are used, namely the eccentricity, roundness, and *Bounding Box*. The last parameter corresponds to the smallest rectangle containing the blob. It is calculated using the ratio between the sides of the rectangle. Ideally, i.e. in the case of a circle, this ratio is 1. In this manner, the parameters are calculated for each blob of the segmented image. If they obey a set of conditions inferred iteratively (eccentricity <0.75, roundness >0.7, *Bounding Box* >0.7) then the blob has a shape approximately circular/elliptical and can therefore be considered a polyp candidate.

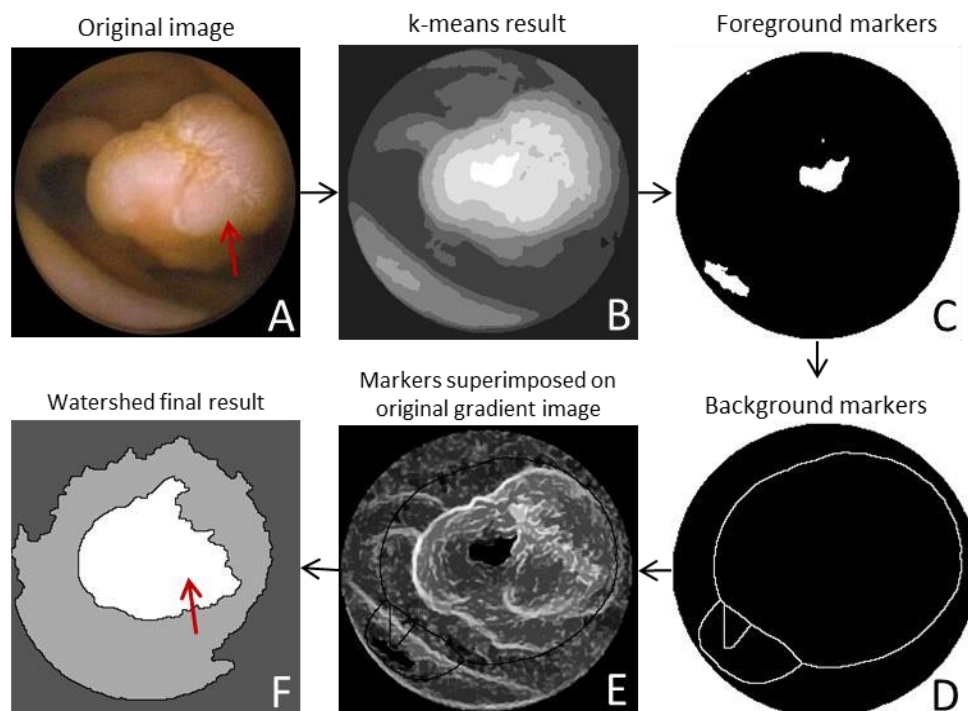


Fig. 4 Polyp segmentation based on marker-controlled watershed technique

After the initial selection of polyp candidates, a 3D reconstruction is also available since it allows a better visualization and perception of mucosal elevations, such as those caused by polyps. The goal of this extra analysis was to help the physicians decide whether or not the detected polyp candidate is an anomaly. In this way, a linear approach of the shape from shading (SFS) algorithm [10] is used, since it is able to recover a shape from a single image by using the gradual variation of shade. The SFS operating principle can be understood under the basis that the direction of the light source is equal to or symmetrical around the viewing direction.

C. Vascularization Detection

NBI technology aims to help clinical professionals in early cancer detection and diagnoses of malignant lesions inside the GIT. In the growth stage of tumors, the number of capillaries in the surface layer of the gastrointestinal wall increases; therefore, the use of NBI is the most effective method for detecting premalignant lesions before the appearance of a tumor. Fig. 5 presents a flowchart in which the main steps of the developed method are shown.

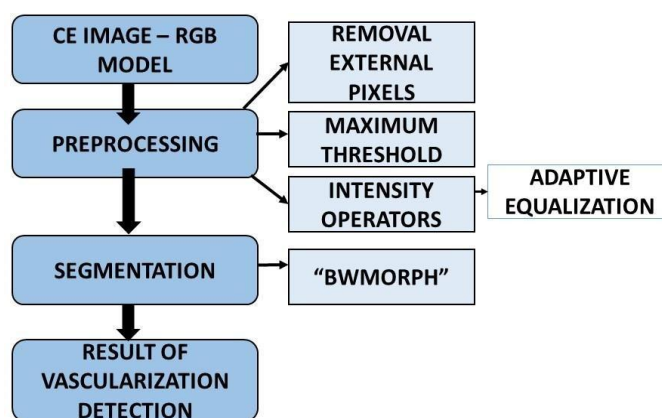


Fig. 5 Flowchart of the developed vascularization detection method

Image pre-processing started with the application of a mask on the original image to remove external pixels around the area of interest. After that, the three color channels (R, G, and B) were split and a maximum threshold value was applied for each channel in order to highlight important details and objects of interest in the foreground, as can be seen in Fig. 6(B).

After the selection of the area of interest, contrast was added to the image in order to highlight relevant details. Afterward, a morphological operation of erosion was applied, and image skeletonization was performed to detach the lines representing the skeleton of the analysis object, as can be seen in Fig. 6(D).

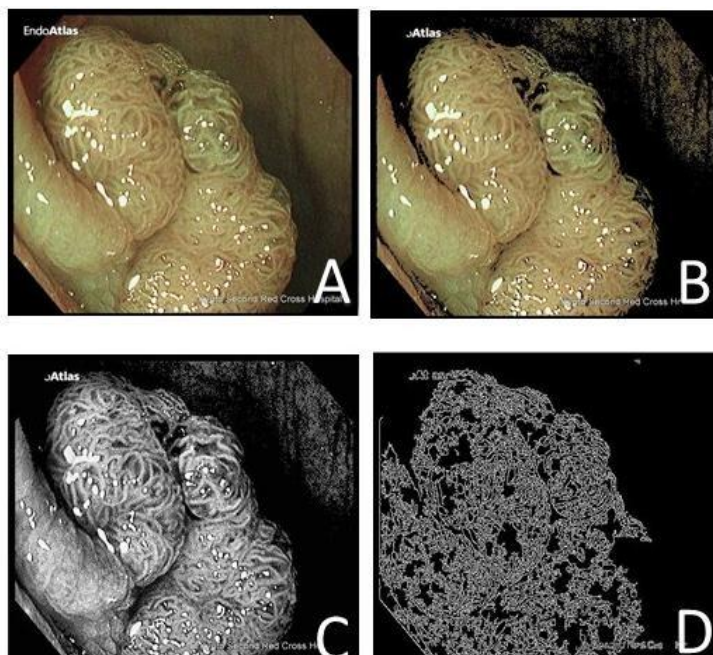


Fig. 6 A) Original image; B) Image after applying the mask for maximum threshold value; C) Image after application of adaptive equalization; D) Image after applying the skeletonization highlight lines

III. RESULTS AND DISCUSSION

A. Bleeding Detection

For the development and validation of this algorithm, 35 images from capsule endoscopy with known diagnoses were used, from which 21 images presented bleeding. Confusion matrixes with the detection results, as well as the sensibility, specificity, and accuracy, can be consulted in Tables 1 and 2.

TABLE 1 CONFUSION MATRIX ASSOCIATED WITH BLEEDING METHOD DETECTION

		Test Outcome	
		Positive	Negative
Real Condition	Bleeding	18	3
	Without Bleeding	4	10

TABLE 2 RESULTS OF STATISTICAL MEASUREMENTS AFTER APPLICATION OF BLEEDING METHOD DETECTION

Result of statistical measurements	
Sensitivity (%)	85.7
Specificity (%)	71.4
Accuracy (%)	80.0

Regarding the images with bleeding, of 21 cases, only 3 images were incorrectly diagnosed; these values correspond to type II errors (False Negatives). These errors should be avoided to prevent misdiagnoses. However, bleeding areas were detected correctly in the other 18 images. Thus, this method demonstrated a sensitivity detection of 86%, meaning most of analyzed images were correctly classified. An example is shown in Fig. 7.

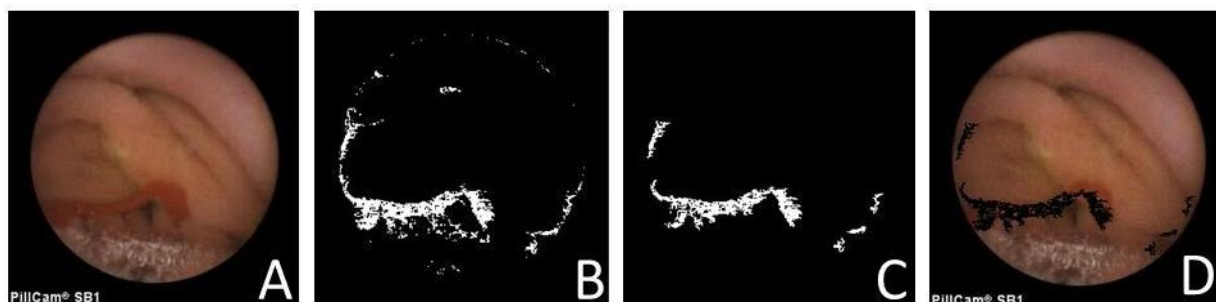


Fig. 7 Application of a bleeding detection method: A) Original image; B) Image before noise removal; C) Image after noise removal; D) Result – image with bleeding

Regarding the images without bleeding, of 14 cases, 10 were correctly classified, which also confirmed the positive results obtained using the developed method. The specificity detection had a satisfactory percentage of around 71%. This result meant that non-bleeding images were detected correctly in most of the cases. The accuracy, which represents the ratio of true results compared to the results obtained, had a very satisfactory result of 80%. Fig. 8 shows an example of a non-bleeding image.

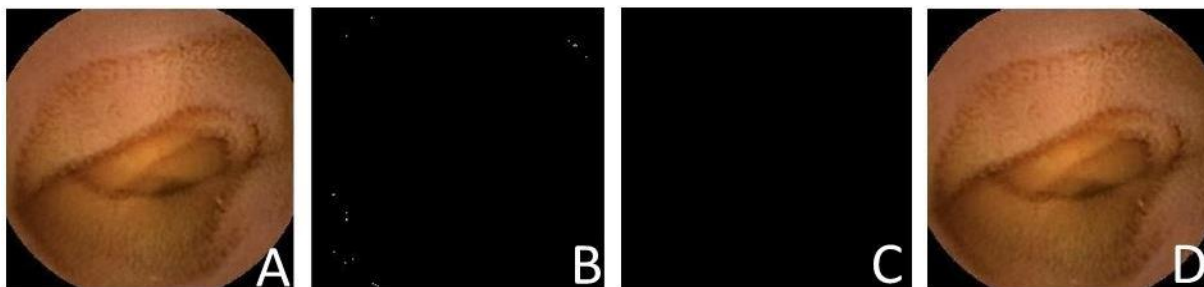


Fig. 8 Application of bleeding detection method: A) Original image; B) Image before noise removal; C) Image after noise removal; D) Result – image without bleeding

Thus, as can be seen from Tables 1 and 2, the results were very positive, meaning this method is able to effectively assist in the early detection of bleeding in the GIT.

B. Polyps Detection

Using a total of 64 EC images from which 35 presented polyps, it was possible to test the performance of the method developed for polyp detection. The method was based on a marker-controlled watershed technique for polyp segmentation (see Fig. 4), and in geometric features for polyp candidate classification. Regarding the segmentation process, as can be seen in Fig. 4(F), the watershed algorithm allows the detection of the polyps' outline in a highly effective manner. Afterwards, the segmented polyps are assessed with geometric measures for classification purposes. These classification results can be consulted on the confusion matrix presented in Table 3. Moreover, the classification accuracy and specificity were also computed, as well as the sensitivity, which illustrates the test's ability to correctly identify a condition, which in this case is the presence of polyps (see Table 4).

The classification accuracy was 77%, while the sensitivity result was 89%. These outcomes are quite positive since it meant that most of the images with polyps were in fact marked as such. In this case, from 35 images with polyps, only 4 were discarded. Hence, there are a reduced number of false negative results, which is desirable in this type of scenario in order to avoid non-detected disorders. On the other hand, the specificity score was 62%, which meant that the number of false positives was rather high, and it would be vital to decrease this percentage in future work. Nevertheless, the overall results were quite satisfactory, and the developed methods were validated.

TABLE 3 CONFUSION MATRIX ASSOCIATED WITH POLYPS METHOD DETECTION

		Test Outcome	
		Positive	Negative
Real Condition	Polyps	31	4
	Without Polyps	11	18

TABLE 4 RESULT OF STATISTICAL MEASUREMENTS AFTER APPLICATION OF POLYPS DETECTION METHOD

Result of statistical measurements	
Sensitivity (%)	88.6
Specificity (%)	62.1
Accuracy (%)	76.6

For further analysis, and in order to help physicians reduce false positive results, a 3D reconstruction technique was also considered using a SFS algorithm based on the linear approach of Tsai, *et al.* [10]. The main purpose of this 3D reconstruction is to enable better visualization and perception of mucosal elevations such as those caused by polyps. Using this algorithm, the 3D reconstruction of individual frames is really impressive because it is possible to obtain shaped structures (surfaces) in detail, including dark areas that are deeper, which explains why this method is used by many authors (see Fig. 9).

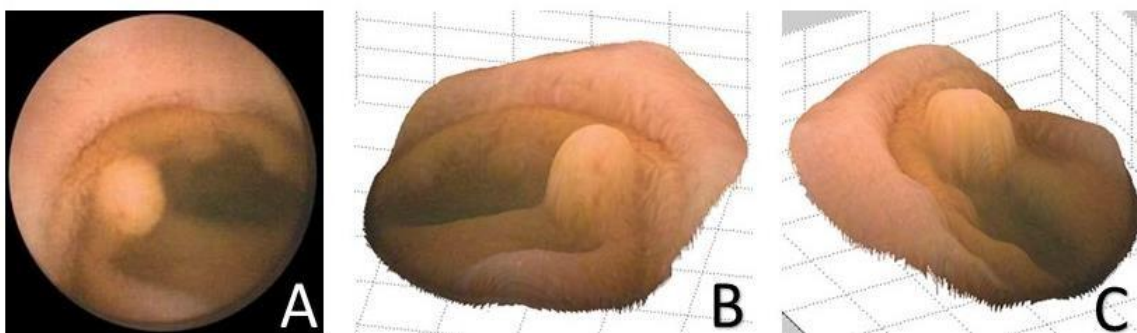


Fig. 9 Polyp 3D reconstruction using a Shape from Shading algorithm

C. Vascularization Detection

Due to the type of analysis, it was not possible to have a quantitative comparison of classification for this method. Nevertheless, to have an evaluation and validation of the developed methodology, the images were divided into 2 groups: images with almost perfect segmentation of the vessels, and images without any segmentation of the vessels. So, for the development and validation of this algorithm, 55 original images from traditional endoscopy were used. Table 5 presents the results that were obtained.

TABLE 5 RESULTS RELATED TO VASCULARIZATION DETECTION

Total Images	Positive Results	Negative Results
55	53	2
Result of statistical measurements		
Rate of Detection (%) = 96.4		
Rate of Non-Detection (%) = 3.6		

The detection rate was 96%, meaning from 55 analyzed images, this method did not detect vascularization in only 2 cases. Thus, the first evaluation of the developed methodology demonstrated that it is able to detect vascularity correctly, as can be seen in Fig. 10.

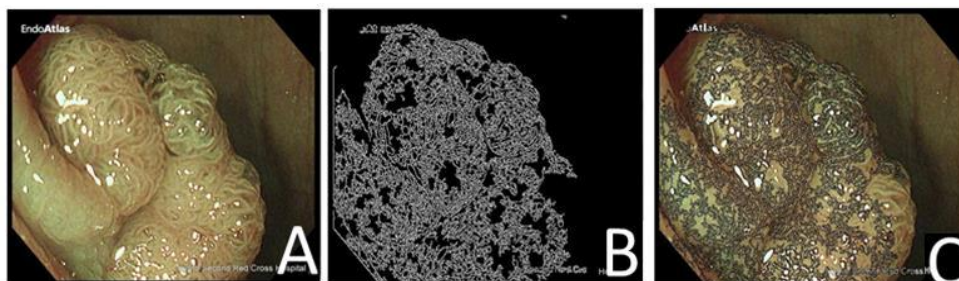


Fig. 10 Application of vascularization detection method

This rate means that in most NBI images, this method is able to successfully detect the underlying vessels in the mucosa with different patterns, and can help in the diagnosis of several pathologies. The presented methods are only the initial analysis and research, and in order to improve this study, it will be necessary to introduce other methods of processing and evaluation.

IV. CONCLUSIONS

This novel endoscopy capsule arose from the need for a less invasive and more reliable diagnostic method for the early detection of gastrointestinal disorders in the GIT. In this paper, the authors proposed new methods for clinical decision support in order to simplify and aid in the early diagnosis of anomalies in the GIT, as well as reduce physicians' fatigue and increase their performance.

The methods presented here focused on the automatic detection of common gastrointestinal disorders, such as polyps and bleeding, which may be early indicators of severe diseases like colorectal cancer. Moreover, other complementary methods were also explored, namely 3D reconstruction of the gastrointestinal mucosa for shape assessment, as well as the use of NBI technology for the analysis of blood vessel patterns. The bleeding detection method was based on identification using a double threshold for each RGB channel, while the polyp detection method used a watershed algorithm for segmentation and geometric features for classification purposes. In both cases, the segmentation and classification results were quite satisfactory. Both algorithms were tested with a considerable amount of ground truth data and, for all of them, an average

percentage of accuracy and sensitivity greater than 75% was obtained. However, it would be possible to lower the percentage of specificity, which measures the proportion of negative cases that are correctly identified as such. Hence, it would be important in a future work to decrease the number of false positives and improve this true negative rate. For 3D reconstructions of the intestinal mucosa, a shape from shading algorithm was employed and very interesting results were observed as this algorithm was capable of performing a detailed reconstruction of the mucosa resorting to only one frame. On the other hand, the automatic detection of vascularization in NBI images was essentially based on the identification of maximum values for each RGB channel. This method is in the early stages of investigation, but the initial results were very promising. In a future stage of research, advances in NBI technology could be useful to combine with the polyp detection method for the identification of malignant polyps since the presence of tumors is often characterized by highly vascularized tissue.

Overall, the methods presented in this research paper obtained satisfactory results and accomplished the goal of supporting the detection of gastrointestinal disorders in EC images. Nevertheless, more work is needed to complete the methods proposed in order to improve the results.

REFERENCES

- [1] (2015) The OMS website. [Online]. Available: <http://globocan.iarc.fr/Default.aspx>.
- [2] D. Bandorski, R. Jakobs, R. Hoeltgen, M. Wieczorek, and M. Keuchel, "Capsule Endoscopy in Patients with Cardiac Pacemakers and Implantable Cardioverter Defibrillators: (Re)evaluation of Current State in Germany, Austria and Switzerland 2010," *Gastroenterology Research and Practice*, vol. 2012, pages 4, 2012.
- [3] H. Ishiguro, S. Saito S, H. Imazu, H. Aihara, T. Kato, and H. Tajiri, "Esophageal Capsule Endoscopy for Screening Esophageal Varices among Japanese Patients with Liver Cirrhosis," *Gastroenterology Research and Practice*, vol. 2012, pages 6, 2012.
- [4] E. Akin, A. Bolat, S. Buyukasik, E. Selvi, and O. Eroy, "Comparison between Capsule Endoscopy and Magnetic Resonance Enterography for the Detection of Polyps of the Small Intestine in Patients with Familial Adenomatous Polyposis," *Gastroenterology Research and Practice*, vol. 2012, pages 5, 2012.
- [5] F. Assirati, C. Hashimoto, R. Dib, L. Fontes, and Navarro-Rodriguez, "Diagnóstico da Doença do Refluxo Gastroesofágico com Endoscopia de Alta Definição e Narrow Band Imaging," *Arquivos Brasileiros de Cirurgia Digestiva*, vol. 27, pp. 59-65, 2014.
- [6] P. Lukes, M. Zabrodsky, J. Plzak, M. Chovanec M, J. Betka, E. Foltynova, and J. Betka, *Endoscopy - Narrow Band Imaging (NBI) - Endoscopic Method for Detection of Head and Neck Cancer*, Chapter 5, pp. 75-87, 2013.
- [7] B. Geavlete, M. Jecu, R. Multescu, and P. Geavlete, "Narrow-Band Imaging Cystoscopy in Non-Muscle-Invasive Bladder Cancer: a Prospective Comparison to the Standard Approach," *Therapeutic Advances in Urology*, vol. 4, no. 5, pp. 211-217, 2012.
- [8] S. Mallick, T. Zickler, D. Kriegman, and P. Belhumeur, "Beyond Lambert: Reconstructing specular surfaces using color," *IEEE Computer Society Conference on Computer Vision and Pattern Recognition*, vol. 2, pp. 619-626, 2005.
- [9] S. Hwang and M. Emre Celebi, "Polyp detection in wireless capsule endoscopy videos based on image segmentation and geometric feature," *IEEE International Conference on Acoustics Speech and Signal Processing*, 2010.
- [10] R. Zhang, P. Tsai, J. Cryer, and M. Shah, "Shape-from-shading: a survey," *IEEE Transactions on Pattern Analysis and Machine Intelligence*, vol. 21(8), pp. 690-706, 1999.